First-in-Class Anti-immunoglobulin–like Transcript 4 Myeloid-Specific Antibody MK-4830 Abrogates a PD-1 Resistance Mechanism in Patients with Advanced Solid Tumors

Lillian L. Siu[1], Ding Wang[2], John Hilton[3], Ravit Geva[4], Drew Rasco[5], Ruth Perets[6,7], Anson K. Abraham[8], Douglas C. Wilson[9], Julia F. Markensohn[8], Jared Lunceford[8], Leah Suttner[8], Shabana Siddiqi[8], Rachel A. Altura[8], and Corinne Maurice-Dror[10]

ABSTRACT

Purpose: In this first-in-human study (NCT03564691) in advanced solid tumors, we investigated a novel first-in-class human IgG4 monoclonal antibody targeting the immunoglobulin-like transcript 4 (ILT4) receptor, MK-4830, as monotherapy and in combination with pembrolizumab.

Patients and Methods: Patients with histologically/cytologically confirmed advanced solid tumors, measurable disease by RECIST v1.1, and evaluable baseline tumor sample received escalating doses of intravenous MK-4830 every 3 weeks as monotherapy (parts A and B) and in combination with pembrolizumab (part C). Safety and tolerability were the primary objectives. Pharmacokinetics, objective response rate per RECIST v1.1, and molecular biomarkers were also evaluated.

Results: Of 84 patients, 50 received monotherapy and 34 received combination therapy. No dose-limiting toxicities were observed; maximum tolerated dose was not reached. MK-4830 showed dose-related target engagement. Eleven of 34 patients in the dose-escalation phase who received combination therapy achieved objective responses; 5 previously had progressive disease on anti–PD-1/PD-L1 therapies. Exploratory evaluation of the association between response and pretreatment gene expression related to interferon-gamma signaling in tumors suggested higher sensitivity to T-cell inflammation with combination therapy than historically expected with pembrolizumab monotherapy, with greater response at more moderate levels of inflammation.

Conclusions: This first-in-class MK-4830 antibody dosed as monotherapy and in combination with pembrolizumab was well tolerated with no unexpected toxicities, and demonstrated dose-related evidence of target engagement and antitumor activity. Inflammation intrinsic to the ILT4 mechanism may be facilitated by alleviating the myeloid-suppressive components of the tumor microenvironment, supporting the target of ILT4 as a potential novel immunotherapy in combination with an anti–PD-1/PD-L1 agent.

Introduction

The development of immune checkpoint inhibitors, including monoclonal antibodies against programmed death 1 (PD-1) or its ligand, programmed death ligand 1 (PD-L1), has improved patient outcomes in those with advanced malignancies; however, many patients do not respond to these therapies or they acquire resistance to them (1). Combining immunotherapies that target distinct mechanisms of immunosuppression may improve outcomes or overcome resistance (1, 2). In addition to the PD-1/PD-L1 axis, which suppresses antitumor effector T-cell responses (3, 4), myeloid-derived suppressor cells (MDSC) represent another major axis of immunosuppression (5) and are associated with poor prognosis in patients with cancer (6). MDSCs dampen T-cell activation, proliferation, and effector responses through numerous mechanisms, including, but not limited to, cytokine production, cell surface receptor signaling, reactive oxygen species production, nutrient deprivation, and regulatory T-cell recruitment (7). Given that MDSCs are a common constituent of the tumor microenvironment and because of their diverse arsenal of suppressive mechanisms, MDSCs are considered a prime target for therapeutic intervention, especially in combination with T-cell–targeted immunotherapy. Several novel therapeutics targeting one or more of these mechanisms have recently been explored in early clinical trials, including molecules targeting colony stimulating factor 1 receptor, CXC chemokine receptors 1/2, adenosine receptors, and class 1 histone deacetylases (8).

[1]Division of Medical Oncology and Hematology, Department of Medicine, Princess Margaret Cancer Center, University of Toronto, Toronto, Ontario, Canada. [2]Department of Medical Oncology, Henry Ford Cancer Institute, Detroit, Michigan. [3]Department of Medicine, The Ottawa Hospital and University of Ottawa, Ottawa, Ontario, Canada. [4]Department of Oncology, Tel Aviv Sourasky Medical Center, Tel Aviv, Israel. [5]Department of Clinical Research, START Center for Cancer Care, San Antonio, Texas. [6]Division of Oncology, Clinical Research Institute at Rambam, Rambam Medical Center, Haifa, Israel. [7]Department of Cancer and Cell Biology, Faculty of Medicine, Technion-Israel Institute of Technology, Haifa, Israel. [8]Oncology Early Development, Merck & Co., Inc., Kenilworth, New Jersey. [9]Department of Profiling and Expression, Genetics and Pharmacogenomics, Merck & Co., Inc., South San Francisco, California. [10]Division of Oncology, Rambam Health Care Campus, Haifa, Israel.

Corrected online March 3, 2022 and August 2, 2022.

Corresponding Author: Lillian L. Siu, Princess Margaret Cancer Center, University of Toronto, 700 University Avenue, Toronto, Ontario, Canada M5G 1Z5. Phone: 416-946-2911; Fax: 416-946-4467; E-mail: Lillian.siu@uhn.ca

Clin Cancer Res 2022;28:57–70

doi: 10.1158/1078-0432.CCR-21-2160

Translational Relevance

MK-4830 plus pembrolizumab was well tolerated and elicited antitumor activity in patients with pretreated advanced solid tumors, including those whose disease previously progressed on immunotherapy. Analysis of tumor response by pretreatment tumor expression of genes related to T-cell inflammation supports the potential for a new mechanism to treat anti–PD-1/PD-L1 resistance. The intriguing data from this study support the further development of MK-4830 in combination with pembrolizumab for patients with advanced solid tumors and the continued investigation into the T-cell and myeloid expression signatures.

Immunoglobulin-like transcript 4 (ILT4) receptor—otherwise known as leukocyte immunoglobulin-like receptor B2 (LILRB2)—is an immunosuppressive member of the immunoglobulin-like transcript (ILT) family that is commonly expressed by many myeloid lineages, including monocytes, macrophages, granulocytes, and dendritic cells (9–12). In the tumor microenvironment, ILT4 is expressed by cells with a phenotype associated with monocytic MDSCs (mMDSC) and granulocytic MDSCs (gMDSC; ref. 13). The prototypical ligand for ILT4 is human leukocyte antigen G (HLA-G), a nonclassical MHC class I molecule expressed by a wide range of tumors; its expression is correlated with poor prognosis (10, 14, 15). Several other ILT4 ligands, including classical human leukocyte antigens (HLA) and angiopoietin-like proteins (12), also may be relevant in driving ILT4-mediated immunosuppression in the tumor microenvironment. Emerging data show that ILT4 antagonism in tumor-associated macrophages (TAM) induces a more proinflammatory state, one that is marked by a shift from the M2-phenotype toward an M1-phenotype (12, 16). Reprogramming TAMs or MDSCs or both to a proinflammatory state may be more advantageous than targeting these cells for depletion because the resultant proinflammatory response from ILT4 inhibition may better stimulate the antitumor T-cell response, particularly in combination with PD-1/PD-L1 blockade (17).

MK-4830 is a fully human monoclonal antibody of the immunoglobulin G4 subclass that specifically binds to ILT4 and blocks its interaction with HLA-G and other ligands (**Fig. 1**; ref. 18). Preclinical data demonstrated that MK-4830 binds to monocytes and granulocytes in the peripheral blood of healthy volunteers and patients with cancer. In a humanized mouse model of cancer, MK-4830 treatment induced significant inhibition of tumor growth (18).

Previous studies have firmly established several tumor-associated biomarkers, including PD-L1, tumor mutational burden (TMB), and microsatellite instability (MSI), that associate with response to the anti–PD-1 antibody pembrolizumab, leading to a more comprehensive and selective treatment paradigm (19). An IFNγ-related, 18-gene, T-cell–inflamed gene expression profile ($Tcell_{inf}GEP$) signature has also been shown to be positively associated with response to pembrolizumab monotherapy in several tumor types (20). Large external databases such as The Cancer Genome Atlas and Merck-Moffitt were used to identify replicable consensus RNA expression signatures intended to be fit-for-purpose signatures representative of canonical pathways associated with tumor biology and tumor microenvironment elements, including a signature related to mMDSCs (21). The mMDSC signature score, when evaluated in joint models with the $Tcell_{inf}GEP$ in a large pan-tumor analysis of patients given pembrolizumab monotherapy ($N = 1{,}118$), showed a modest but statistically significant negative association with objective response, providing clinical evidence that the mMDSC–suppressor cell axis may be a resistance mechanism for pembrolizumab monotherapy (21).

Here, we report efficacy and safety data from the first-in-human phase I trial of MK-4830 as monotherapy and in combination with pembrolizumab in patients with advanced solid tumors. Although the sample size was limited, descriptive evaluation of key pembrolizumab

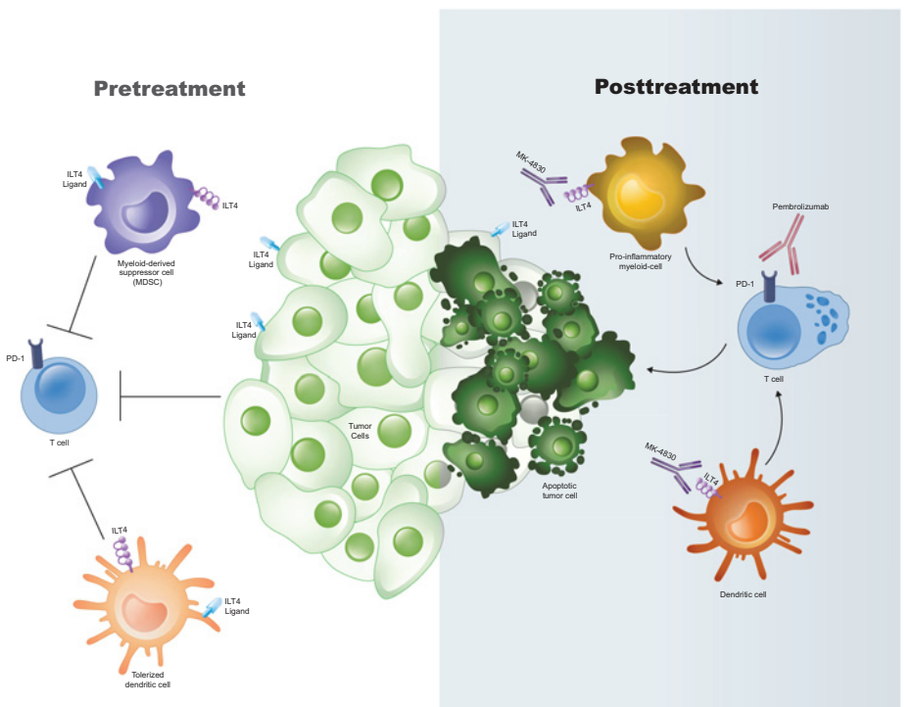

Figure 1.
Proposed mechanism of action of MK-4830. ILT4, immunoglobulin-like transcript 4; PD-1, programmed death 1.

monotherapy biomarkers in the context of combination therapy with MK-4830 is provided because it may be relevant to interpreting the evidence for ameliorating anti–PD-1/PD-L1 resistance in the combination therapy setting.

Patients and Methods

Study design

In this multicenter, open-label, first-in-human, phase I trial, patients were assigned to receive MK-4830 as monotherapy (parts A and B) or in combination with pembrolizumab (part C; ClinicalTrials.gov, NCT03564691). Patients whose disease progressed on monotherapy were eligible to cross over to combination therapy following clinical or radiographical evaluation. This study was conducted in accordance with Good Clinical Practice Guidelines and the Declaration of Helsinki; the protocol (4830–001–03) was approved by the institutional review boards or ethics committees of all participating sites. All patients provided written informed consent to participate before enrollment.

Patient population

Patients (age ≥18 years) had histologically or cytologically confirmed metastatic solid tumors for which no available therapy could convey clinical benefit (previous anti–PD-1/PD-L1 therapy was permitted), measurable disease per Response Evaluation Criteria in Solid Tumors version 1.1 (RECIST v1.1), Eastern Cooperative Oncology Group performance status of 0 or 1, evaluable baseline tumor sample (archived or newly collected), and adequate organ function. Key exclusion criteria included chemotherapy, radiotherapy, or biological anticancer therapy ≤4 weeks before the first dose, discontinuation of any previous immunotherapy regimen because of an immune-related adverse event (AE), previous treatment with another agent targeting ILT4 or HLA-G, chronic systemic steroid therapy (the exception was oral physiological replacements), known untreated central nervous system metastasis or carcinomatous meningitis, and active autoimmune disease.

Treatment

MK-4830 was administered intravenously at a starting dose of 3 mg and subsequent dose escalation to a maximum proposed dose of 1,600 mg every 3 weeks (Q3W). Given the potential for MK-4830 to activate the immune system and the limitations of standard toxicology studies to model these effects in the preclinical setting, a conservative starting dose was chosen to ensure safety. The 3 mg starting dose of MK-4830 was determined on the basis of integration of the data obtained from *in vitro* studies evaluating MK-4830 binding to granulocytes and monocytes obtained from healthy volunteers and patients with cancer (data not shown) and on nonclinical pharmacokinetics and safety and toxicology studies in nonhuman primates. Emphasis was placed on the *in vitro* receptor-binding data because of the lack of target homology, orthologous protein expression, and cross-reactivity of MK-4830 for ILT4 in rodents and nonhuman primates. The maximum proposed dose of 1,600 mg was projected to provide pharmacokinetic exposures in the micromolar range. The highest dose of MK-4830 was expected to provide >90% target receptor occupancy (RO) based on receptor-binding affinity and was to be confirmed by measuring blood RO. Part A of the dose-escalation phase (MK-4830 monotherapy) followed an accelerated titration design (ATD) with 1 to 3 patients treated per cohort with an approximately 3-fold increase between MK-4830 dose levels. The starting dose for part B (MK-4830 monotherapy) was based on safety criteria [dose-limiting toxicity (DLT) or grade ≥2 toxicity] or ≥75% ILT4 RO in peripheral blood mononuclear cells demonstrated at any dose level in part A. Part B of the dose-escalation phase continued using a modified toxicity probability interval (mTPI) design to identify the maximum tolerated dose (MTD) or the maximum-administered dose (MAD) of MK-4830 monotherapy. Enrollment in part C (combination therapy with MK-4830 plus pembrolizumab 200 mg Q3W) was initiated after the first 2 doses in part B were completed. Part C of the dose-escalation phase used the mTPI method to determine the MTD or MAD of MK-4830 in combination with pembrolizumab. Treatment continued until progressive disease (PD), unacceptable AEs, intercurrent illness, investigator/patient decision to withdraw, or 2 years of treatment.

Study outcomes

The primary objective of the dose-escalation phase was to characterize the safety and tolerability of MK-4830 as monotherapy and in combination with pembrolizumab. The secondary objective was to evaluate pharmacokinetic parameters of MK-4830 when administered alone or with pembrolizumab. Tertiary objectives included evaluation or identification of the following: circulating anti–MK-4830 and anti-pembrolizumab antibodies; pharmacokinetics of pembrolizumab administered in combination with MK-4830; objective response rate (ORR) as determined by RECIST v1.1 and immune-related RECIST per investigator (22); and molecular (genomic, metabolic, proteomic, and/or transcriptomic) biomarkers potentially indicative of clinical response or resistance, safety, pharmacodynamic activity, or mechanism of action of MK-4830 as monotherapy and in combination with pembrolizumab. Disease control rate (DCR)—defined as complete response (CR), partial response (PR), or stable disease (SD) with progression-free survival (PFS) duration of ≥6 months—was an unspecified aspect of the analysis.

Safety assessments and imaging

The DLT evaluation period for the monotherapy and combination groups encompassed events that occurred within the first 3 weeks of cycle 1, day 1. Dose finding for parts B and C followed the mTPI design, with a target DLT rate of 30%. Safety was assessed by review of AEs and serious AEs during the study and for 30 days after the last dose if the patient transitioned to a new anticancer therapy or 90 days after the last dose if the patient remained on study. For patients initially assigned to monotherapy, AEs were recorded in the monotherapy group if they occurred while the patient was receiving monotherapy and in the combination therapy group if they occurred after the patient crossed over to combination therapy. AE severity was graded according to the Common Terminology Criteria for Adverse Events version 4.0. Tumor imaging using CT or MRI was performed every 9 weeks until confirmed PD, start of new anticancer therapy, withdrawal of consent, death, or end of study.

Pharmacokinetics, anti-drug antibodies, and target engagement

Serum concentrations of MK-4830 and pembrolizumab were used to derive pharmacokinetic parameters of MK-4830 alone and with pembrolizumab. Blood samples were collected to evaluate levels of circulating anti-drug antibodies (ADA) and to perform pharmacodynamic RO analysis. RO of ILT4 was measured on circulating myeloid cells before and after the administration of MK-4830. Briefly, whole-blood and fresh tumor biopsy samples for ILT4 RO were assessed using fit-for-purpose validated flow cytometry assays to support exploratory biomarker endpoints. A dual detection method was used to measure unoccupied and total ILT4 on the cell surfaces of representative

myeloid cell types before or after MK-4830 administration or at both time points. In blood, $CD45^+/Lin1^-/CD11b^+/CD33^+/HLADR^+$-expressing monocytes were assessed, whereas in fresh tumor samples, only viable $CD45^+/Lin1^-/CD11b^+/CD33^+$-expressing monocytes were assessed because of the variable sample quality.

Biomarker assessments

PD-L1, TMB, $Tcell_{inf}GEP$, and myeloid-specific biomarkers were assessed using archival or newly obtained tumor samples from all patients in the combination group of the study.

PD-L1 protein expression was assessed by immunohistochemistry (IHC) using PD-L1 22C3 IHC pharmDx (Agilent) performed at Interpace Pharma Solutions.

TMB was assessed by DNA extracted from formalin-fixed paraffin-embedded (FFPE) tissue using the Qiagen FFPE kit. DNA fragmentation was performed using the Covaris M220 focused-ultrasonicator with the settings of 75W for peak incident power, 25% as duty factor, 1,000 for cycles per burst, and a treatment time of 6 minutes per sample at 40°C. For the TruSight Oncology 500 (TSO500) next-generation sequencing (NGS) library preparation,

Table 1. Summary of AEs.

AE, *n* (%)	MK-4830 monotherapy[a] *n* = 50		MK-4830 + pembrolizumab[a] *n* = 52	
Any-grade AE	50 (100)		48 (92)	
Grade 3–5	23 (46)		23 (44)	
Led to discontinuation	2 (4)		1 (2)	
Serious	14 (28)		18 (35)	
Serious and led to discontinuation	0		0	
Led to death[b]	2 (4)		0	
Any-grade TRAE	24 (48)		28 (54)	
Grade 3–5	3 (6)		4 (8)	
Led to discontinuation	1 (2)		1 (2)	
Serious	0		4 (8)	
Serious and led to discontinuation	0		0	
Led to death	0		0	
Most common AEs (≥10% incidence)				
AE, *n* (%)	**Any**	**Grade ≥3**	**Any**	**Grade ≥3**
Fatigue	20 (40)	4 (8)	14 (27)	1 (2)
Nausea	14 (28)	0	8 (15)	0
Decreased appetite	11 (22)	1 (2)	14 (27)	0
Diarrhea	10 (20)	0	8 (15)	1 (2)
Abdominal pain	8 (16)	2 (4)	8 (15)	2 (4)
Dyspnea	8 (16)	3 (6)	8 (15)	0
Arthralgia	7 (14)	0	7 (13)	0
Back pain	7 (14)	0	7 (13)	1 (2)
Constipation	7 (14)	0	7 (13)	0
Cough	7 (14)	0	7 (13)	0
Pneumonia	7 (14)	4 (8)	1 (2)	1 (2)
Vomiting	7 (14)	0	11 (21)	0
Pyrexia	6 (12)	0	3 (6)	0
Upper abdominal pain	5 (10)	0	1 (2)	0
Anemia	5 (10)	1 (2)	8 (15)	4 (8)
Dizziness	5 (10)	0	4 (8)	0
Headache	5 (10)	0	6 (12)	0
Peripheral edema	1 (2)	0	9 (17)	0
Hypothyroidism	2 (4)	0	7 (13)	0
Increased blood creatinine	2 (4)	0	6 (12)	0
Most common TRAEs (≥5% incidence)				
Fatigue	6 (12)	1 (2)	7 (13)	1 (2)
Diarrhea	5 (10)	0	2 (4)	1 (2)
Arthralgia	4 (8)	0	3 (6)	0
Increased aspartate aminotransferase	3 (6)	2 (4)	1 (2)	0
Decreased appetite	3 (6)	0	1 (2)	0
Nausea	3 (6)	0	3 (6)	0
Pruritus	3 (6)	0	2 (4)	0
Vomiting	3 (6)	0	1 (2)	0
Hypothyroidism	2 (4)	0	5 (10)	0
Maculopapular rash	2 (4)	0	4 (8)	0

Abbreviations: AE, adverse event; TRAE, treatment-related adverse event.
[a]AEs occurring before crossover are counted in the monotherapy column; AEs occurring after crossover are counted in the combination therapy column.
[b]AEs leading to death were death ($n = 1$) and tumor hemorrhage ($n = 1$).

Table 2. Summary of confirmed tumor response per RECIST v1.1 by investigator assessment.

Confirmed response, *n* (%)	MK-4830 monotherapy *n* = 50	MK-4830 + pembrolizumab *n* = 34	Crossover to MK-4830 + pembrolizumab *n* = 18
ORR	1 (2)[a]	8 (24)[b]	1 (6)[c]
CR	0	1 (3)	0
PR	1 (2)	7 (21)	1 (6)
SD	11 (22)	9 (26)	1 (6)
SD with PFS ≥6 months	5 (1)	6 (18)	0
PD	34 (68)	16 (47)	3 (17)
No RECIST assessment[d]	4 (8)	1 (3)	13 (72)[e]

Abbreviations: CR, complete response; ORR, objective response rate; PFS, progression-free survival; PR, partial response; RECIST v1.1, Response Evaluation Criteria in Solid Tumors version 1.1; SD, stable disease.
[a]Patient had high-grade serous ovarian cancer.
[b]Patients had microsatellite-high colorectal cancer (*n* = 2), gastric cancer (*n* = 2), head and neck squamous cell carcinoma (*n* = 1), Merkel cell carcinoma (*n* = 1), non–small cell lung cancer (*n* = 1), and papillary thyroid (*n* = 1).
[c]Patient had microsatellite-high colorectal cancer.
[d]Includes patients who had the opportunity to have a postbaseline assessment based on the date of their first dose but did not have any postbaseline assessment by the data cutoff date.
[e]Eleven patients have been evaluated by immune Response Evaluation Criteria in Solid Tumors.

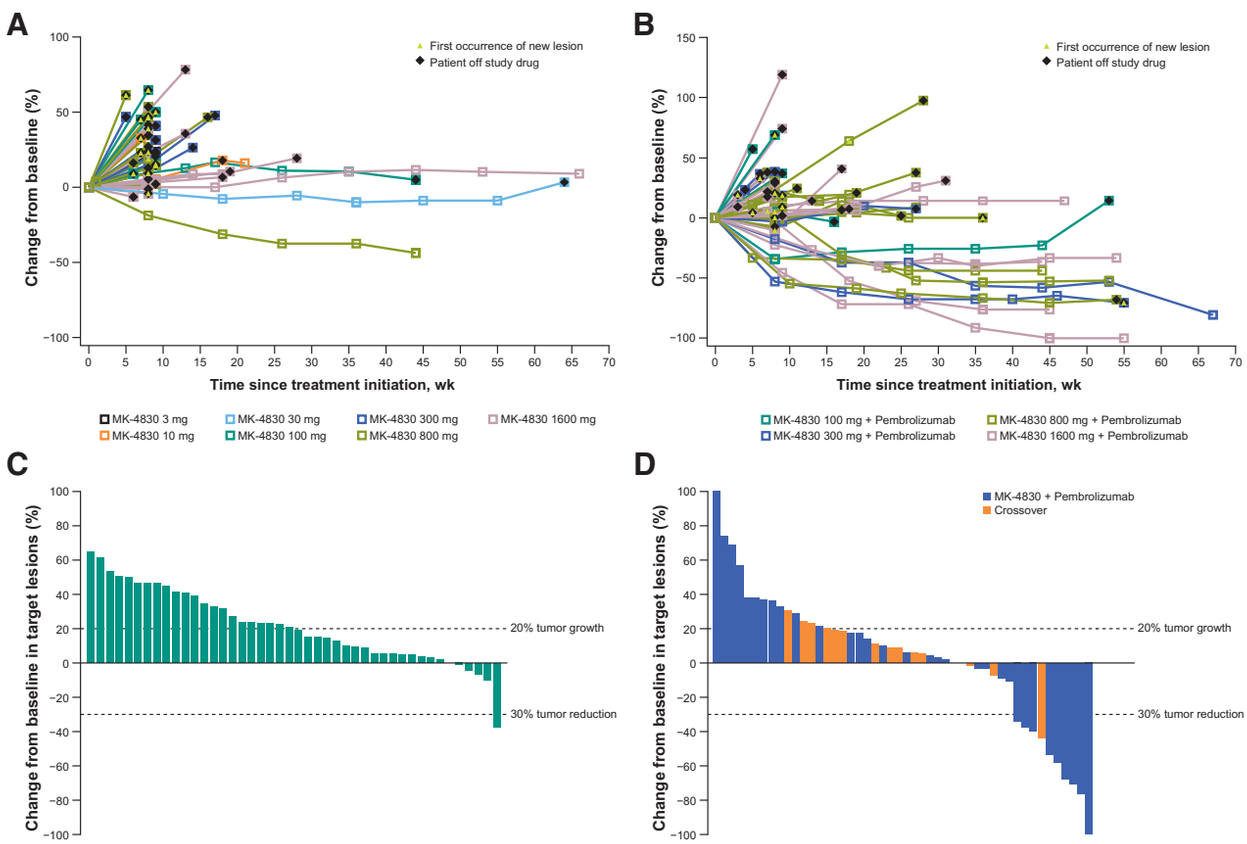

Figure 2.
Target lesion change over time (RECIST v1.1) in patients who received (**A**) MK-4830 monotherapy or (**B**) MK-4830 in combination with pembrolizumab. Best percentage change from baseline in target lesion based on investigator assessment (RECIST v1.1) in patients who received (**C**) MK-4830 monotherapy or (**D**) MK-4830 in combination with pembrolizumab. RECIST v1.1, Response Evaluation Criteria in Solid Tumors version 1.1.

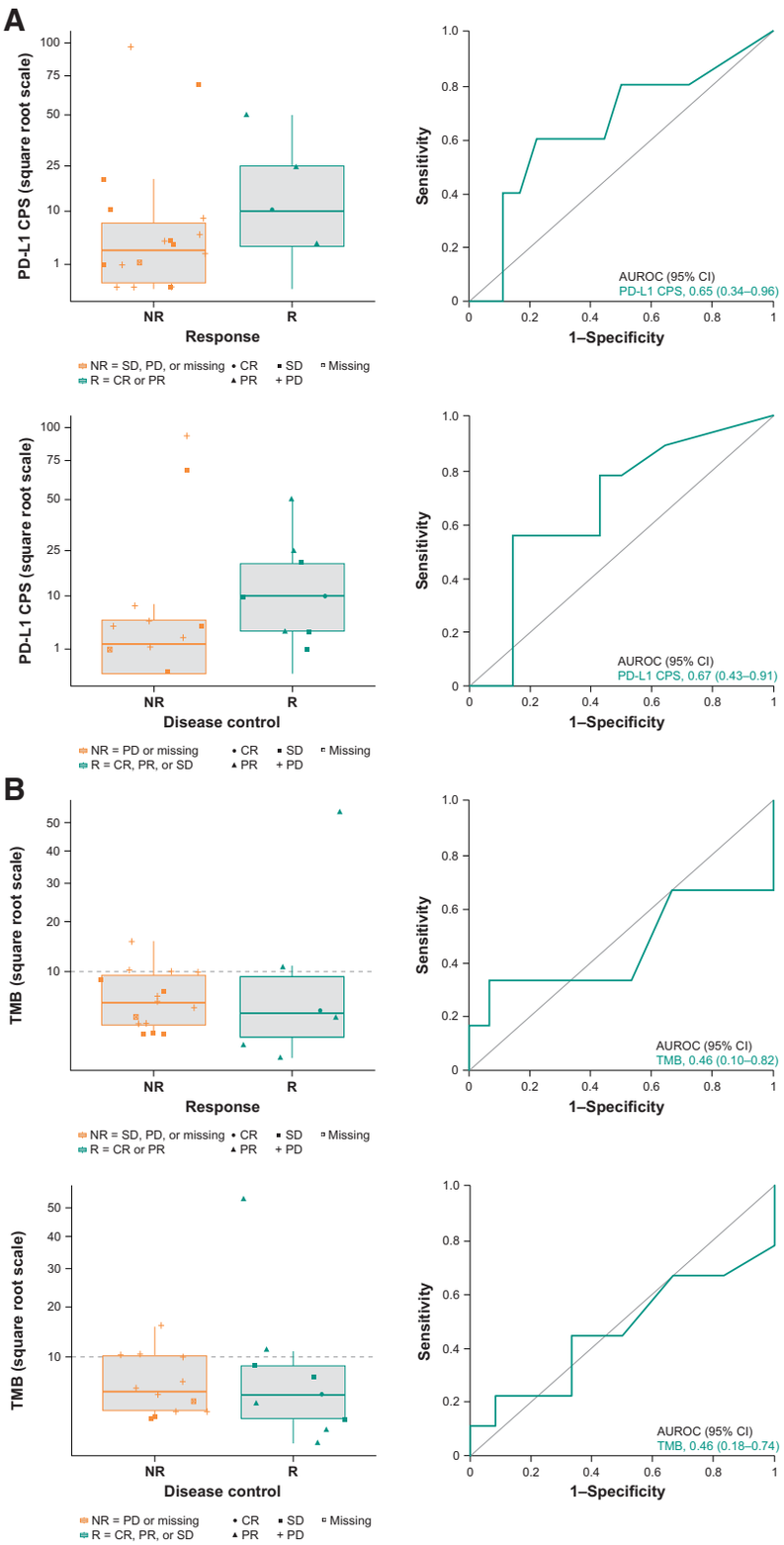

Figure 3.

Association between response and (**A**) PD-L1 status, (**B**) TMB status, and (**C**) $Tcell_{inf}GEP$ score. AUROC, area under the receiver operating characteristic; CI, confidence interval; CPS, combined positive score; CR, complete response; NR, nonresponder; PD, progressive disease; PD-L1, programmed death ligand 1; PR, partial response; R, responder; SD, stable disease; $Tcell_{inf}GEP$, T-cell–inflamed gene expression profile; TMB, tumor mutational burden. (*Continued on the following page.*)

Figure 3.
(*Continued.*)

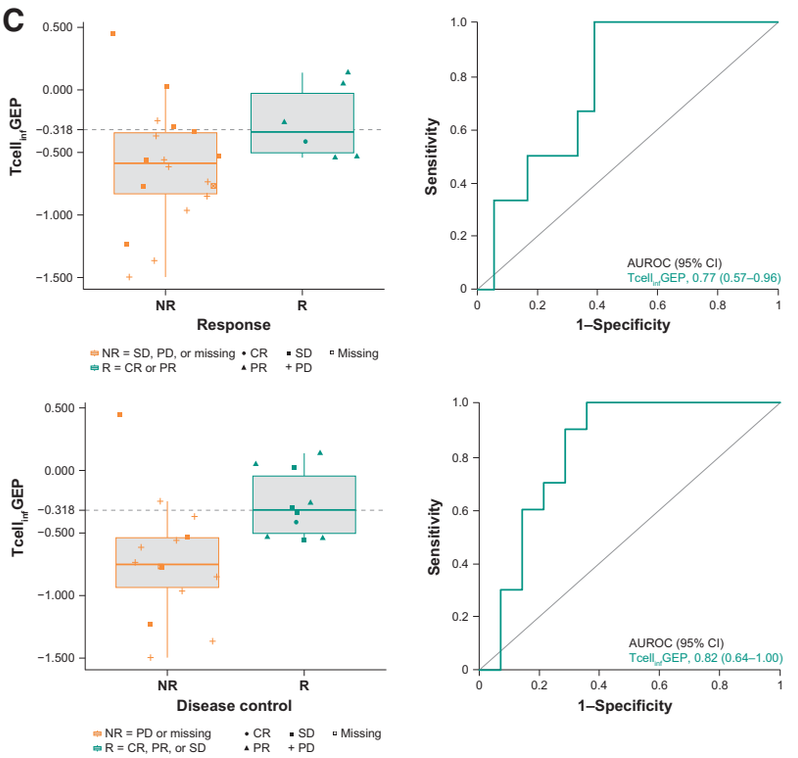

40 to 50 mg FFPE DNA per sample was used. Library preparation was performed manually in accordance with the manufacturer's protocol, with 24 samples per batch. NGS was performed on a NextSeq 550 (Illumina) instrument with 8 libraries per sequencing run. TSO500-TMB was reported using the TSO500 Local App version 1 (Illumina). The manufacturer's quality control criteria were used to determine whether a result was valid, including NGS library concentration of ≥1 ng/μL, median insert size of ≥70 base pairs, median exon coverage of ≥50 count, and percentage of exons with coverage ≥50 count of ≥90%.

$Tcell_{inf}GEP$ and the mMDSC signatures were assessed by RNA extracted from FFPE pretreatment tumor samples using the High Pure FFPE RNA Isolation Kit (Roche) according to the manufacturer's protocol. RNA sequencing was used to measure the 18-gene $Tcell_{inf}GEP$ and the 218 genes of the mMDSC signature. Input sample data were generated using the HiSeq 4000 and the TruSeq RNA Access Library Prep method (Illumina). Gene-level fragments per kilobase million (FPKM) values were generated in Omicsoft Array Studio v11.0 (Qiagen) according to the established RNA sequencing pipeline. Omicsoft sequence aligner as alignment algorithm, Human.B37.3 as alignment reference, and Ensembl.R75 as gene model were used. FPKM values were then converted to $\log_{10}(0.01 + \text{FPKM})$, and each sample was normalized by subtracting the 75th percentile evaluated over probes annotated as protein coding and assigned to chromosomes 1:22, X, and Y. $Tcell_{inf}GEP$ score was calculated according to the published formula as weighted sum over 18 genes using normalized values for the 18 genes and previously published 18-gene coefficients as weights (20). Note that the $Tcell_{inf}GEP$ is calculated as a weighted average of its member genes, whereas the mMDSC signature score is a simple average. Expression of myeloid-specific biomarkers, mMDSC signature score, LILRB2 levels, and HLA-G were also evaluated. As previously described (21), mMDSC signature scores are analyzed by adjusting the data for the $Tcell_{inf}GEP$ relative to the clinical outcome to ensure the score is independent of the $Tcell_{inf}GEP$, which is in line with findings for the mMDSC signature score as a negatively associated factor in joint regression models with the $Tcell_{inf}GEP$ (21). When evaluating patterns of clinical response in the present study, parallel use of the mMDSC signature score was analyzed by adjusting for the $Tcell_{inf}GEP$ by simple linear regression of the expression levels of mMDSC signature scores on the $Tcell_{inf}GEP$ and calculating the residual levels of mMDSC; this evaluates whether these putatively suppressive myeloid-related factors are higher or lower than expectations based on $Tcell_{inf}GEP$. The same approach was used for LILRB2 and HLA-G when comparing levels for responders and nonresponders.

Serum cytokines, including IFNγ, IL1β, IL2, IL4, IL6, IL8, IL10, IL12p70, IL-13, and TNFα, were measured by ELISA. Flow cytometry was also used to quantify circulating levels of monocytes, neutrophils, mMDSCs, polymorphonuclear or granulocytic (PMN)-MDSCs, and early-stage MDSCs as well as T-cell activation. Baseline expression levels of HLA-A, HLA-B, HLA-C, HLA-F, and HLA-G were evaluated in patient tumor samples by RNA sequencing.

Statistical analysis

Safety was evaluated in all patients who received ≥1 dose of study treatment (all-patients-as-treated population), with patients grouped according to the treatment received. The DLT-evaluable population comprised patients who experienced a DLT during the first cycle and those who completed the first cycle of treatment without a DLT. Prespecified DLTs included the following: (i) grade 4 nonhematological toxicity (nonlaboratory); (ii) grade 4 hematological toxicity lasting ≥7 days: grade 4 thrombocytopenia of any duration and/or grade 3 thrombocytopenia associated with clinically significant bleeding; (iii) any nonhematological AE grade ≥3 in severity (exceptions:

grade 3 fatigue lasting ≤3 days; grade 3 diarrhea, nausea, or vomiting without use of antiemetics or antidiarrheals per standard of care; and grade 3 rash without the use of corticosteroids or anti-inflammatory agents per standard of care); (iv) any grade 3 or grade 4 ALT (alanine aminotransferase), AST (aspartate aminotransferase), or bilirubin laboratory values [exception: If AST or ALT was grade 2 at baseline (as in patients with liver metastases), then a DLT was defined as >2× above baseline]; (v) any other nonhematological laboratory value if clinically significant medical intervention was required to treat the patient, or if the abnormality led to hospitalization, persisted for >1 week, or resulted in a drug-induced liver injury (exceptions: clinically nonsignificant, treatable, or reversible laboratory abnormality, including in alkaline phosphatase, gamma glutamyl transferase, or uric acid); (vi) febrile neutropenia grade 3 or grade 4; (vii) prolonged delay (>2 weeks) in initiation of cycle 2 because of treatment-related toxicity; and (viii) any treatment-related toxicity that caused the patient to discontinue treatment during cycle 1. Peripheral blood MK-4830 RO pharmacokinetics and ADAs were summarized by planned visit and time for each dose. ORR and DCR were assessed in the full analysis set, which included patients with measurable disease at baseline who received ≥1 dose of study treatment. The clinical data cutoff date was July 10, 2020.

Availability of data and materials

Merck Sharp & Dohme Corp., a subsidiary of Merck & Co., Inc. (MSD), is committed to providing qualified scientific researchers access to anonymized data and clinical study reports from the company's clinical trials for the purpose of conducting legitimate scientific research. MSD is also obligated to protect the rights and privacy of trial participants and, as such, has a procedure in place for evaluating and fulfilling requests for sharing company clinical trial data with qualified external scientific researchers. The MSD data-sharing website (available at: http://engagezone.msd.com/ds_documentation.php) outlines the process and requirements for submitting a data request. Applications will be promptly assessed for completeness and policy compliance. Feasible requests will be reviewed by a committee of MSD subject matter experts to assess the scientific validity of the request and the qualifications of the requestors. In line with data privacy legislation, submitters of approved requests must enter into a standard data-sharing agreement with MSD before data access is granted. Data will be made available for request after product approval in the United States and the European Union or after product development is discontinued. There are circumstances that may prevent MSD from sharing requested data, including country or region-specific regulations. If the request is declined, it will be communicated to the investigator. Access to genetic or exploratory biomarker data requires a detailed, hypothesis-driven statistical analysis plan that is collaboratively developed by the requestor and MSD subject matter experts; after approval of the statistical analysis plan and execution of a data-sharing agreement, MSD will either perform the proposed analyses and share the results with the requestor or will construct biomarker covariates and add them to a file with clinical data that is uploaded to an analysis portal so that the requestor can perform the proposed analyses.

Results

Patients and baseline characteristics

From July 11, 2018 to July 10, 2020, 99 patients were screened and 84 were treated in the dose-escalation phase of this study (MK-4830 monotherapy, $n = 50$; MK-4830 plus pembrolizumab, $n = 34$; Supplementary Fig. S1). Eighteen patients crossed over from the monotherapy group to receive combination therapy upon radiological confirmation of PD. The median age was 63 years (range, 31–83); most patients (56%) had previously received ≥3 lines of therapy, and 23 patients (27%) had been previously treated with immunotherapy, including anti–PD-1/PD-L1 therapy (Supplementary Table S1).

In the monotherapy group, patients were treated with MK-4830 at the following doses: 3 mg ($n = 2$), 10 mg ($n = 2$), 30 mg ($n = 1$), 100 mg ($n = 7$), 300 mg ($n = 8$), 800 mg ($n = 15$), and 1,600 mg ($n = 15$). In the combination group, all patients received pembrolizumab 200 mg plus MK-4830 at the following doses: 100 mg ($n = 5$), 300 mg ($n = 6$), 800 mg ($n = 8$), and 1,600 mg ($n = 15$).

Median time from cycle 1, day 1 of treatment to data cutoff was 17 months (range, 11–24) in the monotherapy group and 13 months (range, 11–18) in the combination group.

At the data cutoff, median treatment duration was 1 month (range, 0–16) in the monotherapy group and 4 months (range, 0–15) in the combination group; 46 patients (PD, $n = 43$; AE, $n = 2$; patient withdrawal, $n = 1$) and 25 patients (PD, $n = 24$; AE, $n = 1$) discontinued study treatment, respectively.

Safety

No DLTs were observed, and an MTD was not reached in either the monotherapy or the combination therapy group. In the monotherapy group, 50 patients (100%) experienced an AE (**Table 1**); the most common (≥20%) were fatigue (40%), nausea (28%), decreased appetite (22%), and diarrhea (20%; **Table 1**). Treatment-related AEs (TRAE) of any grade occurred in 24 patients (48%; **Table 1**); 3 patients (6%) experienced a total of 7 grade 3 or grade 4 events (fatigue, $n = 1$; increased AST, $n = 2$; increased ALT, $n = 1$; increased blood alkaline phosphatase, $n = 1$; increased blood pressure, $n = 1$; increased gamma-glutamyl transferase, $n = 1$; **Table 1**). One patient (2%) discontinued treatment because of a TRAE (increased AST, grade 2). Of the 52 patients treated with combination therapy ($n = 34$ in part C; $n = 18$ who crossed over from parts A and B), 48 (92%) experienced AEs (**Table 1**); the most common (≥20%) were decreased appetite (27%), fatigue (27%), and vomiting (21%; **Table 1**). TRAEs of any grade occurred in 28 patients (54%; **Table 1**); 4 patients (8%) experienced a grade 3 or grade 4 event (fatigue, $n = 1$; pneumonitis, $n = 1$; hyperglycemia, $n = 1$; hypotension, $n = 1$; **Table 1**). One patient discontinued treatment because of a TRAE (pneumonitis). Four patients (8%) in the combination group experienced a serious TRAE; none led to discontinuation. No treatment-related deaths (grade 5 event) occurred in either treatment group.

Pharmacokinetics/pharmacodynamics

Serum levels of MK-4830 increased with increasing doses (3–1,600 mg; Supplementary Fig. S2A). Increases in MK-4830 doses (3–1,600 mg) resulted in dose-dependent increases in blood ILT4 RO (Supplementary Fig. S2B). The initial MK-4830 monotherapy dose escalation followed an ATD to minimize the number of patients treated at potentially subtherapeutic doses of MK-4830. The 100 mg starting dose for part B, which used the mTPI design with ≥3 patients per dose level, was considered appropriate to ensure some therapeutic benefit based on an average blood percentage RO of ≥60% at MK-4830 C_{trough} (Supplementary Fig. S2B). In part B, an average blood RO of >80% was achieved at dose levels above 300 mg throughout the dosing interval. In patients with available MK-4830 serum pharmacokinetic and blood RO data ($n = 21$), the average blood percentage RO was 96.4% ± 3.62% at the end of cycle 1, that is, cycle 2 predose (day 21

pharmacokinetics showed $C_{trough} = 74.9 \pm 17.9$ μg/mL) at the 800-mg dose level; attempts to quantify tumor ILT4 RO from fresh tumor biopsy samples were not successful. MK-4830 immunogenicity assessment is ongoing, and preliminary results suggest a low incidence of ADAs (data not shown). For MK-4830, a preliminary recommended phase 2 dose of 800 mg Q3W was selected on the basis of the entirety of the data, which included achieving >95% average blood RO in parts B and C of dose escalation.

Tumor response

Eleven of 84 patients (10 confirmed and 1 unconfirmed) with heavily pretreated advanced solid tumors in the dose-escalation phase of the trial achieved an objective response. One of 50 patients in the monotherapy group achieved a confirmed partial response (PR) for an ORR of 2% (**Table 2**); this patient had high-grade serous ovarian cancer and disease progression on 7 previous chemotherapy treatments and received MK-4830 at the 800-mg dose level. Another patient

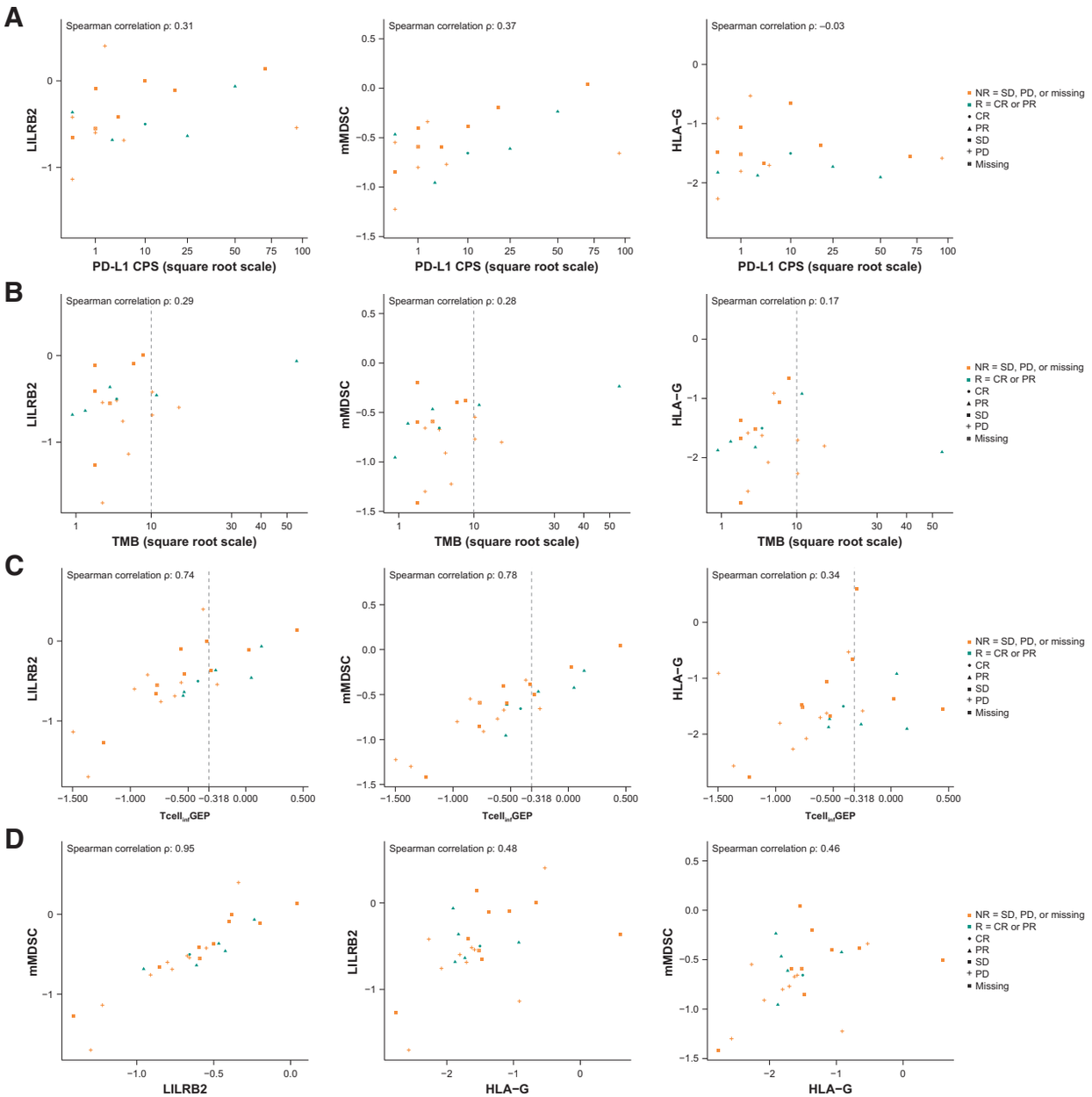

Figure 4.
Correlation between myeloid-specific biomarkers and (**A**) PD-L1 status, (**B**) TMB status, (**C**) $Tcell_{inf}GEP$ score, and (**D**) other myeloid-specific biomarkers. CPS, combined positive score; CR, complete response; HLA-G, human leukocyte antigen G; LILRB2, leukocyte immunoglobulin-like receptor B2; mMDSC, monocytic myeloid-derived suppressor cell; NR, nonresponder; PD, progressive disease; PD-L1, programmed death ligand 1; PR, partial response; R, responder; SD, stable disease; $Tcell_{inf}GEP$, T-cell–inflamed gene expression profile; TMB, tumor mutational burden.

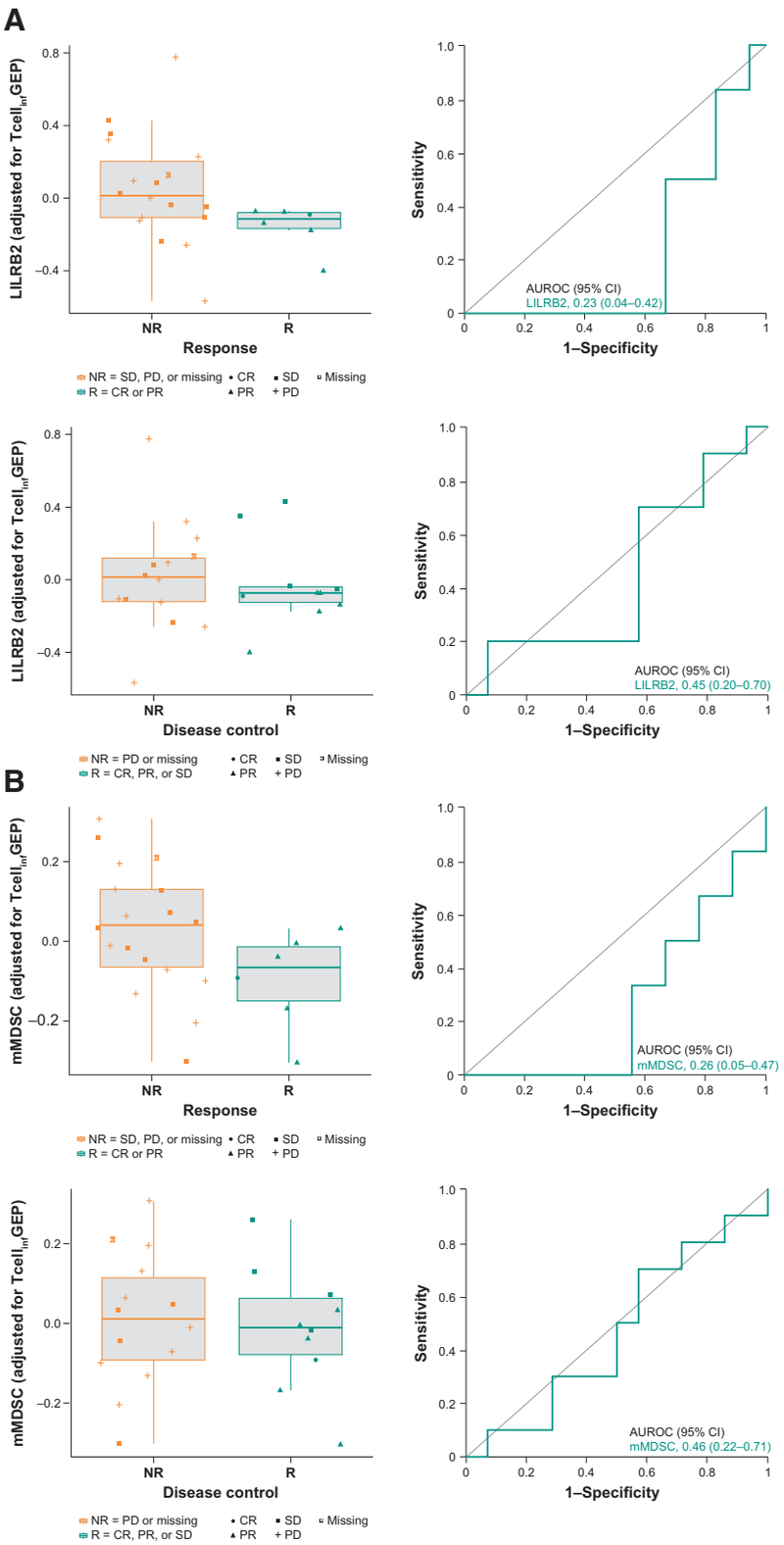

Figure 5.

Association between response and $Tcell_{inf}GEP$-adjusted (**A**) LILRB2, (**B**) mMDSC, and (**C**) HLA-G. AUROC, area under the receiver operating characteristic; CI, confidence interval; CR, complete response; HLA-G, human leukocyte antigen G; LILRB2, leukocyte immunoglobulin-like receptor B2; mMDSC, monocytic myeloid-derived suppressor cell; NR, nonresponder; PD, progressive disease; PR, partial response; R, responder; SD, stable disease; $Tcell_{inf}GEP$, T-cell–inflamed gene expression profile. (*Continued on the following page.*)

Figure 5.
(*Continued.*)

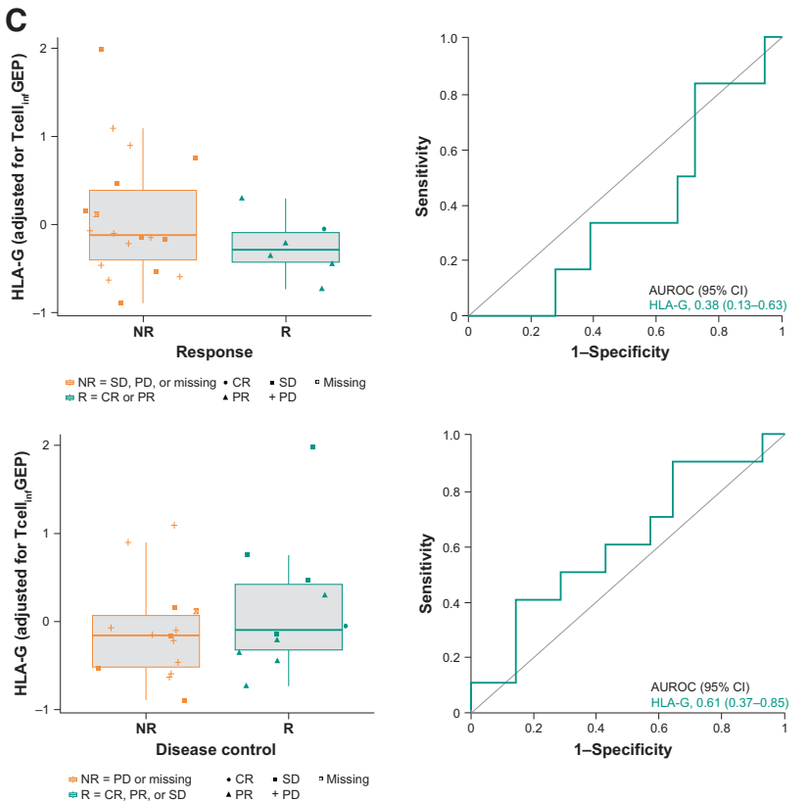

with ovarian cancer in the monotherapy group completed 35 cycles of treatment and had a best overall response of SD. Eight of 34 patients receiving combination therapy achieved a confirmed response (CR, $n = 1$; PR, $n = 7$) and 6 additional patients had SD ≥6 months (per RECIST v1.1 by investigator review) for an ORR of 24% and a DCR of 41% (**Table 2**; Supplementary Table S2). One additional patient in the combination treatment group achieved an unconfirmed PR. In the crossover group, 1 patient with MSI-high colorectal cancer achieved a confirmed PR. Ten patients with a variety of recurrent advanced solid tumors [head and neck squamous cell carcinoma (HNSCC), $n = 2$; gastric cancer, $n = 2$; colorectal cancer, $n = 2$; non–small cell lung cancer (NSCLC), $n = 1$; dendritic sarcoma, $n = 1$; papillary thyroid, $n = 1$; Merkel cell carcinoma, $n = 1$] had continued PRs at doses of MK-4830 100 mg ($n = 1$), 300 mg ($n = 1$), 800 mg ($n = 4$), and 1,600 mg ($n = 4$). A total of 51% of patients with responses previously received ≥3 lines of therapy. In addition, 5 of 11 patients (45%) who achieved a response (4 confirmed and 1 unconfirmed) had previous disease progression on an anti–PD-1/PD-L1 alone or in combination with other agents. All confirmed responses were maintained for ≥6 months (**Fig. 2A** and **B**; Supplementary Fig. S3). Reductions in target lesion size of ≥30% were observed in the patient receiving monotherapy and the 10 patients receiving combination therapy (including those who crossed over; **Fig. 2C** and **D**).

Biomarker analysis

PD-L1

Of the 34 patients in the dose-escalation phase who received combination therapy, 25 [6 responders (CR or PR), 19 nonresponders (SD, PD, or missing, including 5 patients with SD and PFS of ≥6 months)] had evaluable PD-L1 status (**Fig. 3A**). A general trend toward higher tumor PD-L1 combined positive score (CPS) expression was observed in responders. Two patients with confirmed response had a tumor PD-L1 CPS or a tumor proportion score of 0 (1 patient with microsatellite stable gastric cancer and another with NSCLC; data not shown).

TMB

Twenty-one patients [6 responders (CR or PR), 15 nonresponders (SD, PD, or missing, including 5 patients with SD and PFS of ≥6 months)] had evaluable TMB status. No trend toward higher TMB status was observed in patients who responded to study treatment (**Fig. 3B**).

Tcell$_{inf}$GEP

Twenty-four patients [6 responders (CR or PR), 18 nonresponders (SD, PD, or missing, including 4 patients with SD and PFS of ≥6 months)] had evaluable Tcell$_{inf}$GEP scores. The distribution of the Tcell$_{inf}$GEP score was higher in responders than in nonresponders (**Fig. 3C**).

Myeloid-specific biomarkers

Gene expression correlation patterns for myeloid-specific biomarkers LILRB2 (ILT4), HLA-G, and mMDSC signature score against PD-L1, TMB, and Tcell$_{inf}$GEP are shown in **Fig. 4**. The correlation between LILRB2 and mMDSC signature score was very strong, with a Spearman correlation of 0.95; both these biomarkers showed moderate correlations with PD-L1 (Spearman correlation $\rho = 0.31$ and 0.37, respectively), low correlations with TMB (Spearman correlation $\rho = 0.29$ and 0.28, respectively), and strong correlations with Tcell$_{inf}$GEP (Spearman correlation $\rho = 0.74$ and 0.78, respectively). HLA-G also showed moderate

correlations with the mMDSC (Spearman correlation $\rho = 0.46$), LILRB2 (Spearman correlation $\rho = 0.48$), and $Tcell_{inf}GEP$ (Spearman correlation $\rho = 0.34$) but little to no correlations with PD-L1 (Spearman correlation $\rho = -0.03$) or TMB (Spearman correlation $\rho = 0.17$).

Given this high degree of correlation between $Tcell_{inf}GEP$ with mMDSC and LILRB2 levels, we were interested in assessing the distribution of LILRB2, mMDSC, and HLA-G as they relate to response after adjusting for the $Tcell_{inf}GEP$ (**Fig. 5**). The distribution of residual scores trended numerically lower for responders than for nonresponders, with an area under the receiver operating characteristic (AUROC) curve for discriminating objective response of <0.5 for mMDSC and LILRB2; no trends were evident when using DCR as the definition of response.

Additional biomarkers

There were no notable differences in baseline or on-treatment circulating cytokine levels (IFNγ, IL1β, IL2, IL4, IL6, IL8, IL10, IL12p70, IL13, and TNFα) between responders and nonresponders. No evidence of dose-dependent changes was observed among monocytes, neutrophils, mMDSCs, PMN-MDSCs, early-stage MDSCs, and T-cell activation in response to MK-4830 treatment, either in monotherapy or combination therapy. Variable trends with response were observed among the putative ILT4 ligands (HLA-A, HLA-B, HLA-C, HLA-F, and HLA-G); it was unclear whether any individual or combination could be useful as a biomarker for response with this small sample size.

Discussion

In this first-in-human trial, the anti-ILT4 antibody MK-4830 was administered to patients with recurrent advanced solid tumors who previously received an average of three anticancer therapies. At doses ranging from 3 to 1,600 mg Q3W, MK-4830 demonstrated an acceptable safety profile when given as monotherapy and in combination with pembrolizumab. No DLTs or treatment-related deaths were observed, and an MTD was not reached. In the combination therapy group, the rate of grade 3 or grade 4 TRAEs was 8% and the rate of all-cause AEs leading to study discontinuation was 2%. Both the types of TRAEs observed in the MK-4830 monotherapy group and the rate of TRAEs observed in the combination group were similar to those of previous studies with pembrolizumab monotherapy (23, 24). Serum MK-4830 concentration and membrane ILT4 RO increased in a dose-dependent manner in both the monotherapy and the combination therapy groups. At doses of 800 mg or higher, blood ILT4 RO approached complete target saturation throughout the dosing interval (Supplementary Fig. S2B). Low ADA rates for MK-4830 were consistent with ADA rates previously observed in pembrolizumab monotherapy studies (19, 25). For MK-4830, a preliminary recommended phase 2 dose of 800 mg Q3W was selected on the basis of the total data. The overall safety profile of combination therapy with MK-4830 and pembrolizumab underscores its utility over more toxic therapies, such as the addition of cytotoxic chemotherapy or radiotherapy, to overcome immune resistance.

Tumor responses were observed when MK-4830 was administered as monotherapy and in combination with pembrolizumab; 45% of patients achieved a PR with MK-4830 plus pembrolizumab after previous disease progression on an anti–PD-1/PD-L1 alone or in combination with other agents, and 3 responders previously had no response to anti–PD-1/PD-L1 treatment or responded but then experienced disease progression. These findings suggest that MK-4830 is active and may overcome a resistance mechanism to anti–PD-1/PD-L1 therapy.

Interestingly, preliminary biomarker data from this study suggest that some responses occurred in patients whose tumors lacked molecular features typically associated with response to pembrolizumab monotherapy, such as responders who had no detectable expression of tumor tissue PD-L1. One such patient with a diagnosis of HER2–negative microsatellite stable gastric cancer and disease progression on three earlier treatments, including an anti–PD-1/PD-L1 antibody, achieved a prolonged PR with MK-4830 plus pembrolizumab. A second patient with NSCLC and disease progression on five earlier treatments, including the PD-1 inhibitor nivolumab (which elicited no response), achieved a confirmed response with MK-4830 plus pembrolizumab and has continued on treatment for >6 months. Given that both these patients had PD-L1–negative tumors and experienced disease progression with other anti–PD-1/PD-L1 therapies, it is notable that they received lengthy therapeutic benefit with MK-4830 plus pembrolizumab. In addition to these clinical findings, it is noteworthy that the data in our study showed a greater association between $Tcell_{inf}GEP$ and response by way of AUROC in patients treated with MK-4830 plus pembrolizumab than was observed historically in the pan-tumor setting with pembrolizumab monotherapy (21). Furthermore, the response rate among patients with $Tcell_{inf}GEP^{low}$ (using the first tertile as a cutoff to define low and nonlow categories; refs. 20, 26) was higher in this population [18% (3/17) for ORR] than it was in the previously reported pan-tumor analysis [2% (1/45)] with pembrolizumab monotherapy (21). These findings suggest that targeting a myeloid-suppressive axis may increase the cytolytic activity of pembrolizumab at a lower threshold of T-cell inflammation. Sample sizes in the present study were modest, however, and further data are needed to verify such observations.

Ever since initial demonstrations that $Tcell_{inf}GEP$ associates with response to pembrolizumab monotherapy, a persistent puzzle has been the existence of some highly inflamed tumors that do not respond to anti–PD-1/PD-L1 therapy. Studying tumor microenviroment gene expression variations beyond the $Tcell_{inf}GEP$ is the subject of ongoing research. A pooled analysis of a large number of single-arm pembrolizumab studies demonstrated the presence of resistance patterns for monotherapy using signatures for stromal/epithelial–mesenchymal transition/TGF-beta–related expression, angiogenesis, and mMDSC (21). Some of these resistance patterns may operate at different strengths in different tumor types, and evaluation in larger randomized pembrolizumab monotherapy trials will be required for full understanding of the role of these patterns on a tumor-specific basis.

Evaluation of mMDSC-related patterns and ILT4 levels is particularly complicated by their strong correlation to T-cell inflammation. Our position is that the coincident effects of these two forms of inflammation in a chronic setting are best understood by trying to separate their relative contributions with the use of joint statistical modeling. Without this, showing an association between the mMDSC signature or ILT4 levels and tumor response with MK-4830 plus pembrolizumab is difficult to interpret because this association has also been observed with pembrolizumab monotherapy. Joint modeling, which mathematically tests the respective independent components, shows a negative association between the $Tcell_{inf}GEP$–adjusted mMDSC signature score and response in a large pan-tumor analysis (21). However, these pan-tumor findings suggested a subtle effect, and it was only with a large sample size ($N = 1{,}118$) that this effect was statistically significant (21).

Anticipating the role of a biomarker developed in the pembrolizumab monotherapy setting when subsequently evaluated under combination treatment requires careful thinking. The researcher must ask whether trends noted in the pembrolizumab monotherapy setting should become stronger or weaker in the context of an effective combination of immunotherapies. Although our working hypothesis is that the $Tcell_{inf}$GEP–adjusted mMDSC signature score and ILT4 levels should no longer manifest as a biomarker of resistence in the presence of an active anti-ILT4 plus anti–PD-1 combination, the data observed here are far from conclusive. Furthermore, it is unclear whether focus should be on these secondary patterns or on monitoring hallmark monotherapy biomarkers, such as PD-L1, TMB, and $Tcell_{inf}$GEP, to know whether we are observing response rates at lower levels for these biomarkers or overall improvements in their associations with clinical outcomes. These questions will continue to be assessed as further data for this combination therapy accrue.

In the present study, response rates and some biomarker associations observed suggest that MK-4830 may overcome some myeloid compartment–driven resistance mechanisms within the tumor microenvironment to enhance cytolytic T-cell responses in combination with PD-1 blockade. This could occur by a synergistic mechanism whereby MK-4830 blocks HLA-G binding to ILT4, which then repolarizes monocytes to a derepressive phenotype, allowing T cells to enter the tumor microenvironment and pembrolizumab to activate the T cells to kill the tumor cells.

Limitations of this dose-escalation study include the small number of patients, the lower dose levels (<800 mg) of MK-4830 received by many patients, the heterogeneous nature of the tumor types in the patient population, and the wide confidence intervals. Nevertheless, the intriguing data from this study support the further development of MK-4830 in combination with pembrolizumab for patients with advanced solid tumors and the continued investigation into the T-cell and myeloid expression signatures. Expansion cohorts of this study are ongoing in patients with varying tumor types, including pancreatic adenocarcinoma, HNSCC, NSCLC, renal cell carcinoma, gastric cancer, glioblastoma, ovarian cancer, triple-negative breast cancer, and mesothelioma.

Authors' Disclosures

L.L. Siu reports grants from Merck Sharp & Dohme Corp., a subsidiary of Merck & Co., Inc., during the conduct of the study; L.L. Siu also reports personal fees from Arvinas, AstraZeneca, Celgene, GlaxoSmithKline, Janpix, Merck Sharp & Dohme Corp., a subsidiary of Merck & Co., Inc., MorphoSys, Naivre Pharma, Oncorus, Pfizer, Relay Therapeutics, Roche, Rubius Therapeutics, Seattle Genetics, Symphogen, Tessa, Treadwell Therapeutics, and Voronoi, as well as grants from AbbVie, Amgen, Astellas, AstraZeneca, Avid Therapeutics, Bayer, Boehringer Ingelheim, Bristol Myers Squibb, GlaxoSmithKline, Intensity Therapeutics, Karyopharm, Mirati Therapeutics, Novartis, Pfizer, Roche/Genentech, Shattuck Labs, and Symphogen outside the submitted work. L.L. Siu's spouse reports stock ownership in Agios and is a cofounder of Treadwell Therapeutics. J. Hilton reports personal fees from Merck, Bristol Myers Squibb, AstraZeneca, and Novartis; grants and personal fees from Eli Lilly; and grants from GlaxoSmithKline outside the submitted work. R. Geva reports grants from Novartis outside the submitted work. R. Geva also reports honoraria from Bristol Myers Squibb, Eli Lilly, Medison, Roche, Novartis, Janssen, Takeda, MSD, Pfizer, and Merck; advisory/consultancy for Eisai, AstraZeneca, Bayer, MSD, Novartis, BI, BOL Pharma, and Roche; educational grant to institution from Novartis; travel and accommodation expenses from Merck, Bayer, Bristol Myers Squibb, and Medison; and options from BOL Pharma and Pyxis. D. Rasco reports non-financial support from Merck during the conduct of the study. R. Perets reports personal fees from MSD, Karyopharm Therapeutics, BiolineRx, and Simplivia outside the submitted work. A.K. Abraham reports a patent for dosing regimen pending to Merck & Co. Inc., as well as employment with Merck & Co. Inc. D.C. Wilson reports personal fees and other support from Merck & Co. during the conduct of the study; D.C. Wilson has a patent for dosing regimens of anti-ILT4 antibody or its combination with anti–PD-1 antibody for treating cancer pending to Merck Sharp & Dohm Corp. J. Lunceford reports other support from Merck & Co., outside the submitted work. L. Suttner reports a patent for biomarkers associated with response to MK-4830 and pembrolizumab combination treatment in cancer patients pending. C. Maurice-Dror reports personal fees from Pfizer, Biomica, Bristol Myers Squibb, Medison, and Novartis outside the submitted work. No disclosures were reported by the other authors.

Authors' Contributions

L.L. Siu: Conceptualization, data curation, formal analysis, validation, writing–review and editing. **D. Wang:** Data curation, formal analysis, validation, writing–original draft, writing–review and editing. **J. Hilton:** Data curation, validation, writing–review and editing. **R. Geva:** Data curation, validation, writing–review and editing. **D. Rasco:** Data curation, formal analysis, validation, writing–original draft, writing–review and editing. **R. Perets:** Data curation, formal analysis, validation, writing–review and editing. **A.K. Abraham:** Conceptualization, formal analysis, validation, writing–original draft, writing–review and editing. **D.C. Wilson:** Conceptualization, formal analysis, validation, writing–original draft, writing–review and editing. **J.F. Markensohn:** Data curation, formal analysis, validation, writing–original draft, writing–review and editing. **J. Lunceford:** Formal analysis, validation, writing–original draft, writing–review and editing. **L. Suttner:** Conceptualization, formal analysis, validation, writing–review and editing. **S. Siddiqi:** Conceptualization, data curation, formal analysis, validation, writing–review and editing. **R.A. Altura:** Conceptualization, data curation, formal analysis, validation, writing–original draft, writing–review and editing. **C. Maurice-Dror:** Data curation, validation, writing–review and editing.

Acknowledgments

The authors thank the patients and their families and caregivers as well as the primary investigators and site personnel for participating in this study. Medical writing and/or editorial assistance was provided by Kathleen Richards, PhD, Holly C. Cappelli, PhD, CMPP, and Christina Votolo of ApotheCom (Yardley, PA). This assistance was funded by Merck Sharp & Dohme Corp., a subsidiary of Merck & Co., Inc. (Kenilworth, NJ).

The publication costs of this article were defrayed in part by the payment of publication fees. Therefore, and solely to indicate this fact, this article is hereby marked "advertisement" in accordance with 18 USC section 1734.

Note

Supplementary data for this article are available at Clinical Cancer Research Online (http://clincancerres.aacrjournals.org/).

Received June 11, 2021; revised August 10, 2021; accepted September 29, 2021; published first October 1, 2021.

References

1. Pitt JM, Vétizou M, Daillère R, Roberti MP, Yamazaki T, Routy B, et al. Resistance mechanisms to immune-checkpoint blockade in cancer: tumor-intrinsic and -extrinsic factors. Immunity 2016;44:1255–69.
2. Rouas-Freiss N, LeMaoult J, Verine J, Tronik-Le Roux D, Culine S, Hennequin C, et al. Intratumor heterogeneity of immune checkpoints in primary renal cell cancer: focus on HLA-G/ILT2/ILT4. Oncoimmunology 2017;6:e1342023.
3. Hirano F, Kaneko K, Tamura H, Dong H, Wang S, Ichikawa M, et al. Blockade of B7-H1 and PD-1 by monoclonal antibodies potentiates cancer therapeutic immunity. Cancer Res 2005;65:1089–96.
4. Francisco LM, Salinas VH, Brown KE, Vanguri VK, Freeman GJ, Kuchroo VK, et al. PD-L1 regulates the development, maintenance, and function of induced regulatory T cells. J Exp Med 2009;206:3015–29.

5. Fleming V, Hu X, Weber R, Nagibin V, Groth C, Altevogt P, et al. Targeting myeloid-derived suppressor cells to bypass tumor-induced immunosuppression. Front Immunol 2018;9:398.
6. Ai L, Mu S, Wang Y, Wang H, Cai L, Li W, et al. Prognostic role of myeloid-derived suppressor cells in cancers: a systematic review and meta-analysis. BMC Cancer 2018;18:1220.
7. Adah D, Hussain M, Qin L, Qin L, Zhang J, Chen X. Implications of MDSCs-targeting in lung cancer chemo-immunotherapeutics. Pharmacol Res 2016;110: 25–34.
8. De Cicco P, Ercolano G, Ianaro A. The new era of cancer immunotherapy: targeting myeloid-derived suppressor cells to overcome immune evasion. Front Immunol 2020;11:1680.
9. Colonna M, Navarro F, Bellón T, Llano M, García P, Samaridis J, et al. A common inhibitory receptor for major histocompatibility complex class I molecules on human lymphoid and myelomonocytic cells. J Exp Med 1997;186:1809–18.
10. Colonna M, Samaridis J, Cella M, Angman L, Allen RL, O'Callaghan CA, et al. Human myelomonocytic cells express an inhibitory receptor for classical and nonclassical MHC class I molecules. J Immunol 1998;160:3096–100.
11. Fanger NA, Cosman D, Peterson L, Braddy SC, Maliszewski CR, Borges L. The MHC class I binding proteins LIR-1 and LIR-2 inhibit Fc receptor-mediated signaling in monocytes. Eur J Immunol 1998;28:3423–34.
12. Gao A, Sun Y, Peng G. ILT4 functions as a potential checkpoint molecule for tumor immunotherapy. Biochim Biophys Acta Rev Cancer 2018;1869: 278–85.
13. Köstlin N, Ostermeir AL, Spring B, Schwarz J, Marmé A, Walter CB, et al. HLA-G promotes myeloid-derived suppressor cell accumulation and suppressive activity during human pregnancy through engagement of the receptor ILT4. Eur J Immunol 2017;47:374–84.
14. Cai Z, Wang L, Han Y, Gao W, Wei X, Gong R, et al. Immunoglobulin-like transcript 4 and human leukocyte antigen-G interaction promotes the progression of human colorectal cancer. Int J Oncol 2019;54:1943–54.
15. Li Q, Li J, Wang S, Wang J, Chen X, Zhou D, et al. Overexpressed immunoglobulin-like transcript (ILT) 4 in lung adenocarcinoma is correlated with immunosuppressive T-cell subset infiltration and poor patient outcomes. Biomark Res 2020;8:11.
16. Chen HM, van der Touw W, Wang YS, Kang K, Mai S, Zhang J, et al. Blocking immunoinhibitory receptor LILRB2 reprograms tumor-associated myeloid cells and promotes antitumor immunity. J Clin Invest 2018;128: 5647–62.
17. Sharma MD, Rodriguez PC, Koehn BH, Baban B, Cui Y, Guo G, et al. Activation of p53 in immature myeloid precursor cells controls differentiation into Ly6c(+) CD103(+) monocytic antigen-presenting cells in tumors. Immunity 2018;48: 91–106.
18. Zuniga L, Joyce-Shaikh B, Wilson D, Cherwinski H, Chen Y, Jeff G, et al. Preclinical characterization of a first-in-class ILT4 antagonist, MK-4830. J ImmunoTher Can 2018;6:115.
19. KEYTRUDA® (pembrolizumab) injection, for intravenous use. Merck Sharp & Dohme Corp.: Whitehouse Station, NJ, USA; 2021.
20. Ayers M, Lunceford J, Nebozhyn M, Murphy E, Loboda A, Kaufman DR, et al. IFN-gamma-related mRNA profile predicts clinical response to PD-1 blockade. J Clin Invest 2017;127:2930–40.
21. Cristescu R, Nebozhyn M, Zhang C, Albright A, Kobie J, Huang L, et al. Pan-tumor analysis of the association of cancer and immune biology-related gene expression signatures with response to pembrolizumab monotherapy. J ImmunoTher Can 2019;7:282.
22. Seymour L, Bogaerts J, Perrone A, Ford R, Schwartz LH, Mandrekar S, et al. iRECIST: guidelines for response criteria for use in trials testing immunotherapeutics. Lancet Oncol 2017;18:e143–e52.
23. Garon EB, Rizvi NA, Hui R, Leighl N, Balmanoukian AS, Eder JP, et al. Pembrolizumab for the treatment of non–small cell lung cancer. N Engl J Med 2015;372:2018–28.
24. Robert C, Schachter J, Long GV, Arance A, Grob JJ, Mortier L, et al. Pembrolizumab versus ipilimumab in advanced melanoma. N Engl J Med 2015;372: 2521–32.
25. van Vugt MJH, Stone JA, De Greef R, Snyder ES, Lipka L, Turner DC, et al. Immunogenicity of pembrolizumab in patients with advanced tumors. J Immunother Can 2019;7:212.
26. Cristescu R, Mogg R, Ayers M, Albright A, Murphy E, Yearley J, et al. Pan-tumor genomic biomarkers for PD-1 checkpoint blockade-based immunotherapy. Science 2018;362:eaar3593.